

## Atom-based stabilization for laser-pumped atomic clocks

V. Gerginov<sup>1,\*</sup>, V. Shah<sup>2</sup>, S. Knappe<sup>2</sup>, L. Hollberg<sup>3</sup>, and J. Kitching<sup>3</sup><sup>1</sup>*Department of Physics, University of Notre Dame, Notre Dame, IN 46556*<sup>2</sup>*Department of Physics, University of Colorado, Boulder, CO 80309 and*<sup>3</sup>*Time and Frequency Division, National Institute of Standards and Technology, Boulder, CO 80305*

Progress towards simplification and improvement of the long-term stability of chip-scale atomic clocks is presented. The conventional technique of laser optical frequency and cell temperature control is compared with a novel technique which avoids the use of temperature sensors. The technique results in a simpler setup and improved long-term performance. Here, laser frequency, laser intensity, RF modulation index and vapor cell atomic density are stabilized using exclusively information from the atoms in the vapor cell. Different feedback schemes for laser intensity and frequency stabilization, as well as cell temperature control are experimentally compared. Their relevance to future design of chip-scale devices is discussed.

## I. INTRODUCTION

Chip-scale atomic clocks (CSACs) with volumes of several cubic millimeters [1] and power consumption below 10 mW [2] have recently been introduced and are expected to provide precise timing in GPS receivers, network applications, and portable instrumentation systems. Integration of a chip-scale physics package with low-power local oscillator (LO) [3] of similar size and control electronics of cubic centimeter size seems possible [4].

Most CSACs are based on a coherent population trapping (CPT) scheme [5], using a vertical cavity surface emitting laser (VCSEL) to excite alkali atoms contained in a small buffer gas vapor cell [6]. The laser injection current is modulated by the LO, which produces sidebands in the optical spectrum of the laser. When the frequency difference between two components in the optical spectrum matches the frequency splitting of the atomic ground state, the optical field pumps part of the atoms into a state that absorbs less light. The decreased absorption is used to stabilize the LO frequency to the atomic transition.

The splitting of the atomic ground state can change due to the AC Stark effect. It is influenced by the optical field parameters such as optical frequency, total intensity, and intensity distribution among the spectral components of the light field. Another factor is the pressure of the buffer gas inside the cell, which depends on the cell temperature. A change in any of these parameters leads to a corresponding change in the LO frequency and to degradation of the clock performance.

The laser wavelength [7], intensity and modulation properties [8, 9] are very sensitive to temperature and injection current. When the laser optical frequency is stabilized by controlling the injection current, the laser intensity becomes coupled to its temperature through the injection current. Changes in the LO out-

put power, RF coupling between the LO and the laser, or the laser modulation parameters (due to temperature, injection current or aging) all will lead to change in the optical field parameters which affect the clock frequency.

The cell temperature determines the buffer gas pressure, which affects the atomic ground state splitting through collisions. Through the use of a mixture of buffer gases, the sensitivity of the clock frequency to cell temperature can be reduced [10, 11]. This reduction is effective only in a limited temperature range because of the nonlinear behaviour of the clock frequency shifts with temperature for different gases.

The goal of the present work is to study the long-term frequency stability of CSAC devices and suggest design changes in both the physics package and control implementation that could lead to better performance under typical field-operated conditions. We describe a novel method, that uses the atomic absorption for stabilization of the optical field parameters and vapor cell temperature. In the conventional method the laser substrate temperature, laser optical frequency, LO output power and temperature of the cell exterior are stabilized. Here, the actual parameters that determine the clock frequency - laser intensity, optical frequency, intensity distribution among the spectral components, and the atomic absorption - are stabilized, which results in better long-term device performance and a simpler design. The new design makes the device largely insensitive to changes in the ambient temperature by eliminating temperature sensors and the thermal gradients associated with their usage.

## II. EXPERIMENTAL SETUP

## A. Conventional setup

The experiment is based on the physics package of a conventional chip-scale atomic clock design developed at NIST [12]. A VCSEL die [7], emitting in a single mode at 795 nm is used to excite the  $D_1$  line ( $5s^2S_{1/2} \rightarrow 5p^2P_{1/2}$ ) transition in  $^{87}\text{Rb}$ . It is

\*Electronic address: gerginov@nist.gov

mounted on a quartz substrate with a deposited thin-film heater. The laser substrate temperature is around  $80^{\circ}\text{C}$  (stabilized to  $\sim 1$  mK using a thermistor and a temperature controller). The thermistor temperature coefficient is  $\sim -4\%/K$ . The LO modulates the laser injection current at one half of the ground state splitting of the Rb atoms (6.835 GHz). The LO output power is chosen so that the first-order sidebands are maximized. The divergent and linearly polarized laser beam passes through a neutral density filter and a quarter-wave plate before entering the  $^{87}\text{Rb}$  vapor cell of  $1\text{ mm}^3$  internal volume. The optical frequency of the laser carrier is tuned such that the first-order sidebands are in resonance with the two ground state components and it is locked to the maximum of the first-order sideband absorption.

The micromachined vapor cell is filled with isotopically enriched  $^{87}\text{Rb}$  and a buffer gas mixture of argon and neon at total pressure of 16 kPa. The cell temperature is maintained in the vicinity of  $85^{\circ}\text{C}$  with 1 mK precision using a thermistor equivalent to the one used for laser temperature control. The optical absorption of the first-order modulation sidebands in the laser optical spectrum is  $\sim 20\%$ .

The LO frequency is stabilized to the  $F = 1$ ,  $m_F = 0 - F = 2$ ,  $m_F = 0$  ground state hyperfine resonance. The CPT resonance has a linewidth of  $\sim 7$  kHz and an absorption contrast (defined as the CPT signal amplitude divided by the optical absorption of the first-order sidebands) of 3.3 %.

The conventional setup is shown in Figure 1 (a).

A fractional frequency instability plot is shown in Figure 1 (filled squares). The long-term stability is limited to  $\sim 5 \times 10^{-11}$  at 200 s.

## B. Laser temperature stabilization using atomic resonances

A problem in the conventional stabilization scheme (Figure 1 (a)) results from varying temperature gradients between the laser p-n junction and temperature sensor. These gradients change with the ambient temperature. This leads to variations in the laser temperature, and correspondingly, to changes in the laser injection current because of the optical frequency lock. Variations in the laser injection current lead to changes in the laser intensity, and instability of the clock frequency due to the AC Stark shift. A simple setup that stabilizes directly the laser p-n junction temperature is shown in Figure 1 (b). The setup is used to keep the laser frequency locked to the optical resonance by controlling the laser temperature. The laser is operated with a constant DC injection current with a superposed AC modulation at 17 kHz. The AC current modulation produces a corresponding laser frequency modulation which results in amplitude modulation after the frequency dependent optical absorption of the vapor cell. As the laser

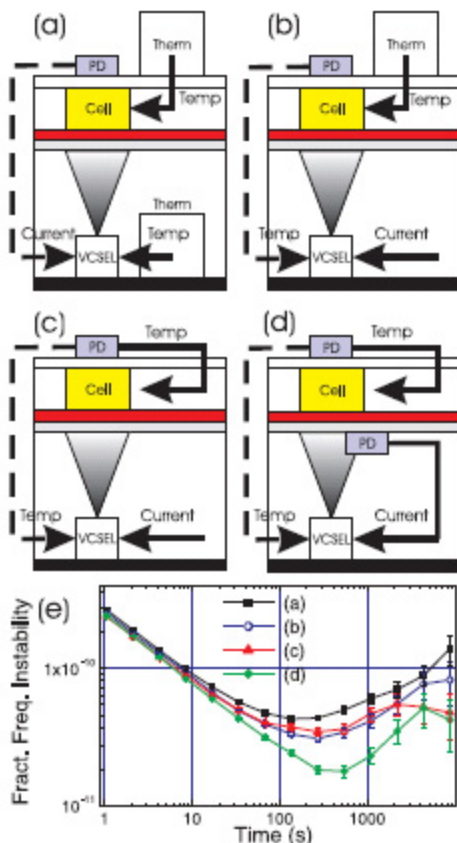


FIG. 1: Top - Experimental setup for CSAC parameter control. Solid lines represent DC signals and dashed lines represent phase detection signals. (a) Conventional setup, Section II A. (b) Laser frequency is controlled using temperature feedback, Section II B (c) Cell temperature is controlled using atomic absorption, IIC (d) Laser intensity is controlled using a photodetector, IID. Bottom - fractional frequency instability plots corresponding to cases (a) through (d).

frequency changes (due to temperature changes or aging, for example) the demodulated photodetector signal can be fed back to the laser thin-film heater to adjust the laser temperature for constant frequency feedback. The bandwidth of the temperature control is limited to  $\sim 30$  Hz. The stability of the laser frequency is estimated to be  $\sim 20$  MHz, or 1 % of the linewidth of the absorption line, and is similar to that obtained with the conventional setup based on thermistor. A fractional frequency instability for the microwave clock transition is shown in Figure 1 (open

circles). It is clear that the reduced feedback bandwidth does not degrade the clock short-term stability and that this method of laser stabilization results in improved clock frequency stability ( $\sim 3.5 \times 10^{-11}$  at 200 s).

### C. Temperature stabilization of the vapor cell using optical absorption

A second problem with the conventional stabilization scheme (Figure 1 (a)) results from varying temperature gradients between the sensor measuring the cell temperature, and the cell interior. As a consequence, a change in the ambient temperature leads to varying temperature of the buffer gas. The Rb vapor density is a strong function of the temperature and so the optical absorption, and hence the light intensity transmitted through the cell, also depends on the cell temperature. Under typical operating conditions, we have change in the absorption of 1%/K, similar to the change in the resistance of a typical thermistor. The DC signal of the photodetector placed behind the cell is a measure of the cell temperature and is used to stabilize it in the setup shown in Figure 1 (c). A fractional frequency instability plot is shown in Figure 1 (solid triangles).

### D. All-optical laser frequency and intensity stabilization

The experimental setup for simultaneous laser intensity and frequency stabilization is shown in Figure 1 (d). The DC signal from the lower photodetector is used to stabilize the laser intensity using a current feedback. The laser beam transmitted through the cell is detected with a second photodetector. The DC signal from the upper photodetector is used to stabilize the cell temperature. The fractional frequency deviation is plotted in Figure 1 (solid diamonds). The stability of  $2 \times 10^{-11}$  at 200 s achieved with this system is improved by more than a factor of two over the frequency stability measured with the conventional setup of Figure 1 (a) using thermistors in a controlled laboratory environment, with changes in the ambient temperature of less than 2 K. At the same time, this technique simplifies the setup, since no thermistors are required, in contrast with previous work [13, 14].

The laser temperature is determined by the stability of the optical lock and the stability of the laser injection current. For 20 MHz optical frequency stability and  $10^{-4}$  injection current stability, the laser temperature is stable to better than 2 mK. The cell temperature is determined by the stability of the voltage references used to control the DC signal on the two photodetectors ( $\Delta V/V \sim 10^{-4}$ ), the optical absorption (20%), and the dependence of the optical absorption on temperature (1%/K). The stability of

the cell temperature is on the order of 50 mK. These stabilities are expected to be largely independent of ambient temperature, since no temperature sensors are used in the setup shown in Figure 1 (d).

## III. FIRST-ORDER SIDEBANDS AMPLITUDE STABILIZATION

In the experiments described above, a synthesizer with a very stable output power was used to modulate the VCSEL injection current. In portable CPT atomic clocks, the synthesizer is replaced with a compact low-power local oscillator (see, for example, [3]). Changes in the output power of the LO redistributes the optical power among the modulation sidebands. This, in turn, can change the clock frequency due to AC Stark shifts from the resonant and off-resonant sidebands. We find that the modulation index changes also with the laser temperature. The laser impedance is modified, and with it, the RF modulation index because of the different RF coupling. To illustrate this, the laser temperature was varied, and the RF power, applied to the VCSEL input in order to make the first-order optical sidebands intensity equal to 50% of the total laser intensity, was measured. The laser carrier was kept in resonance with  $5s^2S_{1/2} F_g = 1 \rightarrow F_e = 1, 2$  transition by a simultaneous change of the laser current. The results are shown in Figure 2.

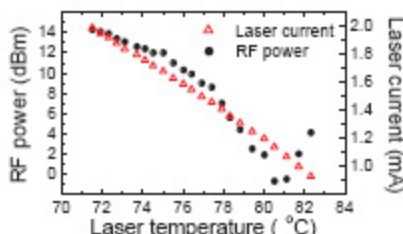


FIG. 2: RF power applied to the VCSEL input in order to make the first-order optical sidebands intensity equal to 50% of the total laser intensity, as a function of the laser temperature (circles). The laser injection current (triangles) was changed simultaneously with the laser temperature to keep the carrier in resonance with  $5s^2S_{1/2} F_g = 1 \rightarrow F_e = 1, 2$  transition.

It is clear that the RF power coupled to the laser has a strong nonlinear behaviour [8, 9], especially at injection currents close to the laser threshold (0.6 mA for the laser used here).

With the laser frequency and intensity stabilized as shown in Figure 1 (d), the remaining parameter that determines the AC Stark shift is the intensity distribution among the different spectral components. For laser frequency modulation, the fraction of output power contained in the first-order sidebands goes

through a maximum at a certain modulation index, and this can be used to maintain consistent modulation index. Since the first-order sidebands are resonant with the optical transitions, their power change will produce a change in the total atomic absorption.

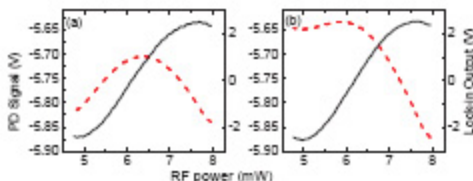


FIG. 3: Photodetector output (dashed) and error signal (solid) as a function of RF power coupled to the laser. Left plot - laser frequency locked using laser temperature. Right plot - laser frequency locked using injection current feedback. The RF power is linearly scanned for 1 s, resulting in RF power change of 40%. The AM modulation was 3% and lock-in amplifier time constant 100 ms.

Figure 3 shows the absorption change detected as a function of the LO output power. The difference between the photodetector signals is due to the way the laser frequency is locked. When thermistors are used, the RF power heats the p-n junction locally, the thermistor doesn't compensate this heating, and the laser power changes through the frequency lock. When the laser frequency is locked to the optical transition using temperature feedback, such local p-n junction heating is compensated by the laser heater, the intensity stays constant and the PD signal changes only because of the changes in the amplitude of the first-order sidebands. This clearly demonstrates the sensitivity of the technique described in Section II B to local temperature variations.

A method is described in Refs. [15–17], where the clock frequency is made insensitive to changes of laser intensity by choosing the RF modulation index such that the AC Stark shifts of each individual spectral component compensate each other. As shown [18], this works well in a narrow laser temperature region and does not provide active control of LO output power changes, RF coupling and laser diode aging.

When the amplitudes of the carrier and sidebands are fixed, and laser power and frequency are stabilized using the experimental setup from Figure 1 (d), the

total AC Stark shift of the clock frequency is "frozen" because the optical frequency and intensity of each spectral component are constant. This approach is a powerful method to minimize clock frequency drifts due to changes in the light field of the laser. In contrast to the method suggested in References [15–17], it is immune to several systematic effects connected with the temperature control of the laser and effects from laser aging. Also, the CPT signal is optimized since it is produced by the two first-order sidebands which contain the maximum intensity available using laser frequency modulation.

#### IV. CONCLUSIONS

A new method is realized for laser frequency and power control without the use of temperature sensors. The clock physics package is simplified and allows for active stabilization of the laser power. Absorption cell temperature stabilization is based on optical attenuation measurements. This simplifies the experimental setup significantly and gives a direct measure of the vapor density inside the cell. All-optical implementation simultaneously stabilizes the laser power, frequency and RF modulation index - the parameters that determine the AC Stark shift of the clock frequency. Under fixed laser intensity and frequency, the clock frequency shows improved clock stability. Initial results of stabilizing the RF modulation index are obtained. This method provides the possibility for full control over the laser light field in a simple and compact way, and shows a great promise for chip-scale atomic devices, and could be implemented in other laser-based frequency standards.

#### Acknowledgments

This work was supported by the Microsystems Technology Office of the U.S. Defense Advanced Research Projects Agency (DARPA). This work is a contribution of NIST, an agency of the U.S. government, and is not subject to copyright.

#### V. REFERENCES

- [1] S. Knappe, L. Liew, V. Shah, P. D. D. Schwindt, J. Moreland, L. Hollberg, and J. Kitching, *Appl. Phys. Lett.* **85**, 1460 (2004).
- [2] R. Lutwak, J. Deng, W. Riley, M. Varghese, J. Leblanc, G. Tepolt, M. Mescher, D. K. Serkland, K. M. Geib, and G. M. Peake, in *Proc of the 36th Precise Time and Time Interval (PTTI) Systems and Applications Meeting* (Reston, Virginia, USA, 2004).
- [3] A. S. Brannon, J. Breitbarth, and Z. Popovic, in *IEEE MTT-S 2005 International Microwave Symposium* (Long Beach, California, USA, 2005).
- [4] G. Gerginov, S. Knappe, P. D. D. Schwindt, V. Shah, L. Liew, J. Moreland, H. G. Robinson, L. Hollberg, and J. Kitching, in *Proc. 2005 Joint Mtg. IEEE Intl.*

- Freq. Cont. Symp. and PTTI Meeting* (Vancouver, Canada, 2005).
- [5] E. Arimondo, *Prog. Opt.* XXXV(35), 257–354 (1998).
- [6] L. A. Liew, S. Knappe, J. Moreland, H. Robinson, L. Hollberg, and Kitching, J., *Appl. Phys. Lett.* 84(14), 2694–2696 (2004).
- [7] H. J. Unold, M. Grabberr, F. Eberhard, F. Mederer, R. Jäger, M. Riedl, and K. J. Ebeling, *Electron. Lett.* 35, 1340–1341 (1999).
- [8] S. Kobayashi, Y. Yamamoto, Y. Ito, and T. Kimura, *IEEE J. Quantum Electron.* QE-18(4), 582–595 (1982).
- [9] P. N. Melentiev, M. V. Subbotin, and V. I. Balykin, *Laser Physics* 11(8), 891–896 (2001).
- [10] W. Happer, *Rev. Mod. Phys.* 44(2), 169–249 (1972).
- [11] J. Vanier and C. Audoin, *The Quantum Physics of Atomic Frequency Standards*, 1st ed. (Adam Hilger, Bristol, UK, 1989).
- [12] J. Kitching, S. Knappe, M. Vukicevic, L. Hollberg, R. Wynands, and W. Weidmann, *IEEE Trans. Instrum. Meas.* 49(6), 1313 – 1317 (2000).
- [13] S. Yamaguchi and M. Suzuki, *IEEE J. Quantum Electron.* 19(10), 1514–1519 (1983).
- [14] D. E. Janssen and M. W. Levine, US Patent 6,222,424 (2001).
- [15] J. Vanier, A. Godone, and F. Levi, in *Proc. Joint Meeting of Eur. Forum on Time and Frequency / Int. Freq. Control. Symp.*, pp. 96–99 (1999).
- [16] M. Zhu and L. Cutler, in *Proc of the 39th Precise Time and Time Interval (PTTI) Systems and Applications Meeting*, pp. 311–324 (Reston, Virginia, USA, 2000).
- [17] M. Zhu and S. Cutler, U.S. Patent 6,201,821 (2001).
- [18] V. Gerginov, S. Knappe, P. D. D. Schwindt, V. Shah, and J. Kitching, *J. Opt. Soc. Am. B* 23(4), 593–597 (2006).